



*Anal. Bioanal. Chem. Res., Vol. 6, No. 1, 47-57, June 2019.*

## Simple and Sensitive Photoluminescent Detection of Meropenem Using Cit-Capped CdS Quantum Dots as a Fluorescence Probe

Naser Samadi\* and Saeedeh Narimani

*Department of Chemistry, Faculty of Science, Urmia University, Urmia, Iran*

*(Received 14 June 2018, Accepted 27 August 2018)*

We have developed water soluble CdS quantum dot (QD) probes for detection of meropenem by using safe and low cost materials. The citrate (Cit) capped CdS QDs are highly stable in aqueous solution and applied for selective and ultrasensitive meropenem (MPN) sensing. The fluorescence intensities of CdS QDs were decreased linearly with increasing MPN in the wide range of  $6 \times 10^{-10}$ - $2.1 \times 10^{-3}$  M. The limit of detection for meropenem determination was 0.5 nM. There was no significant wavelength shift on the fluorescence-quenched signals in the presence of the drug. The effect of common foreign ions and drugs on the fluorescence of the QDs was studied to evaluate the selectivity, and the results showed a high selectivity of the Cit capped CdS QDs towards MPN. The validity of this method was confirmed by high performance chromatography method (HPLC). The method presented here is simple, rapid, low cost, sensitive, inexpensive and suitable for practical applications.

**Keywords:** CdS quantum dots, Fluorescence probe, Drug, Meropenem

### INTRODUCTION

Colloidal semiconductor nanocrystals or quantum dots (QDs), such as CdS, CdSe and CdTe, have emerged as an attractive fluorescent material in the past two decades because of their advantageous intrinsic properties such as wide absorbance range, narrow signals in emission spectra, size-tunable, symmetric band emission, high quantum yield and excellent photostability [1-6]. These unique properties of QDs show considerable advantages over traditional organic fluorophores [7] in the application of analytical chemistry, resulting in the increased use of QDs in various areas [8-13]. QDs have been used as photoluminescent sensors, biological luminescent labels [14-16], bioimaging [17,18], medicine, analytical chemistry, especially in sensors [19-21].

Determination of drugs have been widely studied [22-26], meropenem (MPN), is a new parenteral carbapenem antibiotic (Fig. 1). It has a very broad spectrum of

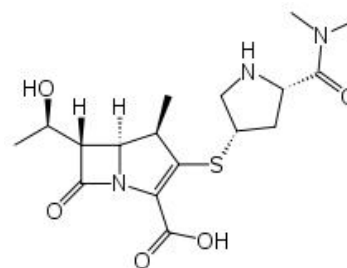


**Fig. 1.** The chemical structure of meropenem. Systematic (IUPAC) name of meropenem is: (4R, 5S, 6S)-3-[5-(Di methyl carbamoyl) pyrrolidin-2-yl] sulfanyl-6-(1-hydroxyethyl)-4-methyl-7-oxo-1-azabicyclo[3.2.0] hept-2-ene-2-carboxylic acid.

antibacterial activity against the majority of Gram-positive and Gram-negative pathogens [27]. Meropenem is more active *in vitro* as compared with Enterobacteriaceae and Pseudomonas aeruginosa, but less active against Gram-positive cocci [28]. Meropenem has shown clinical efficacy

\*Corresponding author. E-mail: samadi76@yahoo.com

in treatment of a wide range of serious infections such as respiratory tract infections and intra-abdominal infections [29,30]. Several methods have been reported for the determination of MPN and its main metabolite in biological fluids, including high performance liquid chromatography (HPLC) [31-34] and capillary zone electrophoresis [35]. Meropenem has been measured in pharmaceutical dosage form only by high performance liquid chromatography (HPLC) method [33,36]. Therefore, accurate and reliable determination of trace amounts of MPN in biological samples is very important for the assurance of consumers' health. In this work, a simple, rapid, selective and sensitive method like spectrofluorimetric measurement was developed for determination of meropenem, in which the quenching properties of QDs were used in sensing of meropenem with high sensitivity and good selectivity.

## EXPERIMENTAL

### Reagents

All used materials were of analytical grade. The metal salts  $\text{Cd}(\text{NO}_3)_2 \cdot 4\text{H}_2\text{O}$ ,  $\text{Na}_2\text{S} \cdot 5\text{H}_2\text{O}$ , sodium citrate,  $\text{Na}_2\text{SO}_4$ ,  $\text{LiCl}$ ,  $\text{NaNO}_3$ ,  $\text{KNO}_3$ ,  $\text{Mg}(\text{NO}_3)_2 \cdot 6\text{H}_2\text{O}$ ,  $\text{Ca}(\text{NO}_3)_2 \cdot 4\text{H}_2\text{O}$ ,  $\text{Fe}(\text{NO}_3)_3 \cdot 9\text{H}_2\text{O}$ ,  $\text{BaCl}_2 \cdot 2\text{H}_2\text{O}$ ,  $\text{Co}(\text{NO}_3)_2 \cdot 4\text{H}_2\text{O}$ ,  $\text{Ni}(\text{NO}_3)_2 \cdot 6\text{H}_2\text{O}$ ,  $\text{MnCl}_2 \cdot 4\text{H}_2\text{O}$ ,  $\text{Cu}(\text{NO}_3)_2 \cdot 3\text{H}_2\text{O}$ ,  $\text{HgCl}_2$ ,  $\text{Pb}(\text{NO}_3)_2$ ,  $\text{Zn}(\text{NO}_3)_2 \cdot 4\text{H}_2\text{O}$ ,  $\text{Cr}(\text{NO}_3)_3 \cdot 9\text{H}_2\text{O}$ ,  $\text{AgNO}_3$ ,  $\text{SnCl}_2$ ,  $\text{Sr}(\text{NO}_3)_2$  purchased from Merck (Germany). Meropenem was purchased from Sigma-Aldrich (Germany). A 0.01 M phosphate buffer solution (PBS) was prepared using  $\text{KH}_2\text{PO}_4$  and  $\text{K}_2\text{HPO}_4$  and used as the medium for QD solutions. All solutions were prepared using doubly distilled, deionized water (DIW).

### Apparatus

Fluorescence spectra were measured on a JASCO-FP-6500PC spectrofluorimeter. UV-Vis absorption spectra were recorded by a computerized WPA-Biowave II instrument using a 10 mm quartz cell. The pH was measured with a Metrohm 827 pH lab pH-meter. The morphology and structure of QDs were investigated by high resolution transmission electron microscopy (HRTEM) and IR spectrometry using a Philips-CM 30 model under the accelerating voltage of 300 KV, and a nexus 670 FT-IR

Thermo Nicolet spectrometer using KBr disk, respectively. The HPLC data were measured in Agilent 1100 series HPLC system having a tunable absorbance detector and injector with 20  $\mu\text{l}$  loop volume. Agilent chemstation software was used for data collecting and processing. Chromatography system (with the terms specified in Table 1) equipped with pump, sample, column, UV detector and recorder. The UV-Vis, wavelength range 190-1100 nm, 1 nm high resolution, double beam, 1 cm length quartz, coated optics was used for the spectral measurements.

### Synthesis of Cit-capped CdS QDs

Citrate capped CdS QDs were prepared using a simple and rapid procedure according to the reference [37] with some modifications. To a 40 ml of solution containing  $1.90 \times 10^{-3}$  M  $\text{CdNO}_3 \cdot 4\text{H}_2\text{O}$  and  $9 \times 10^{-3}$  M sodium citrate, 0.1 M NaOH was added to adjust the pH of the solution to 7.5. The solution was then purged with pure nitrogen for 30 min, then, 10 ml of a  $4 \times 10^{-3}$  M  $\text{Na}_2\text{S}$  solution was added, and the mixture reacted at room temperature for 30 min under pure nitrogen. The concentration of the synthesized Cit-capped CdS nanocrystals was  $8 \times 10^{-4}$  M. By replacing sodium citrate with thioglycolic acid or cysteine, thioglycolic acid and cysteine-capped CdS QDs were synthesized. The colloidal quantum dots were stored in a refrigerator. No precipitation was observed over 1 month.

### Real Sample Preparation

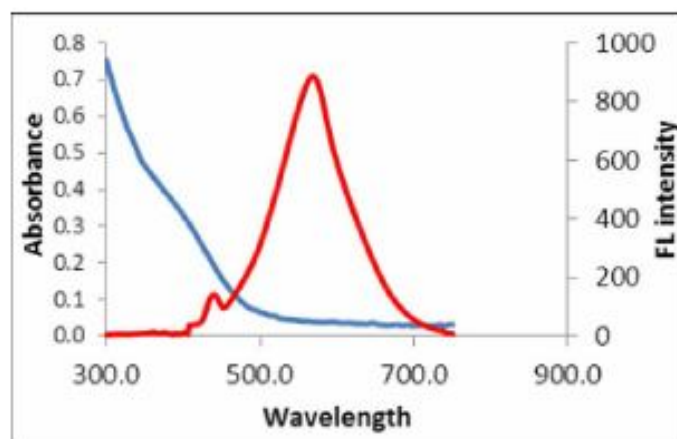
For human urine analysis, urine sample of a healthy volunteer was collected and centrifuged (9000 rpm, 15 min) to precipitate impurities. Then, the supernatant was diluted with deionized water in the ratio of 1:10 and collected. The experiments were carried out by a standard addition method.

### Determination of Meropenem by Cit-CdS QDs

The fluorescence quenching of the Cit-CdS QDs by MPN was performed in the phosphate buffer solution at pH = 6. 1.0 ml of the Cit-CdS solution, 1.0 ml of PBS (pH = 6.0) and a certain amount of meropenem was sequentially added to a 3 ml calibrated test tube. The mixture was diluted to volume with ultrapure water, shaken thoroughly and equilibrated about 10 min. The fluorescence intensity was measured at  $\lambda_{\text{em}} = 567$  and  $\lambda_{\text{ex}} = 380$  nm. The fluorescence intensity of Cit-CdS QDs was assigned as  $I_0$ . The

**Table 1.** Optimized HPLC Condition

Parameter	Specification
Stationary phase	C18 ODS HyperSil
Mobile phase	Water with 0.2% triethylamine pH (6): Acetonitrile (20:80)
Flow rate (ml min <sup>-1</sup> )	1.0 ml min <sup>-1</sup>
Temperature (°C)	Ambient
Detection wavelength	225 nm

**Fig. 2.** The absorption and fluorescence spectra of Cit-CdS QDs.

fluorescence intensity after adding MPN was assigned as  $I$ . The fluorescence ratio ( $I/I_0$ ) was plotted versus the concentration of MPN to obtain a calibration curve.

## RESULTS AND DISCUSSION

### Characterization of the Cit-capped CdS QDs

Absorption and emission spectra of Cit-CdS QDs are shown in (Fig. 2). The wide absorption spectra can be seen in the range of ultraviolet wavelengths around 380 nm. The corresponding emission spectra at 380 nm showed the maximum fluorescence intensity at 567 nm. The fluorescence spectrum shape exhibited a symmetric and narrow spectrum signifying that the Cit-CdS QDs were

nearly homogeneous and monodisperse. The effect of sodium sulfide on the fluorescence intensity of the QDs has been previously investigated. Therefore, Cit-CdS QDs were synthesized with different concentrations of Na<sub>2</sub>S using the same procedure. The fluorescence spectra in each sodium sulfide concentration are shown in (Fig. 3A). With decreasing the amount of Na<sub>2</sub>S the fluorescence intensity of the resulted QDs was decreased and fluorescence spectra were broader than those of the initial used concentration. The red shift in the emission peak resulting from an increase in concentration of Na<sub>2</sub>S indicates the growth of particles to larger size. The results showed that when concentration of Na<sub>2</sub>S is  $4 \times 10^{-3}$  M the fluorescence spectra were narrow and symmetric. As shown by Fig. 3B, UV radiation of CdS QDs

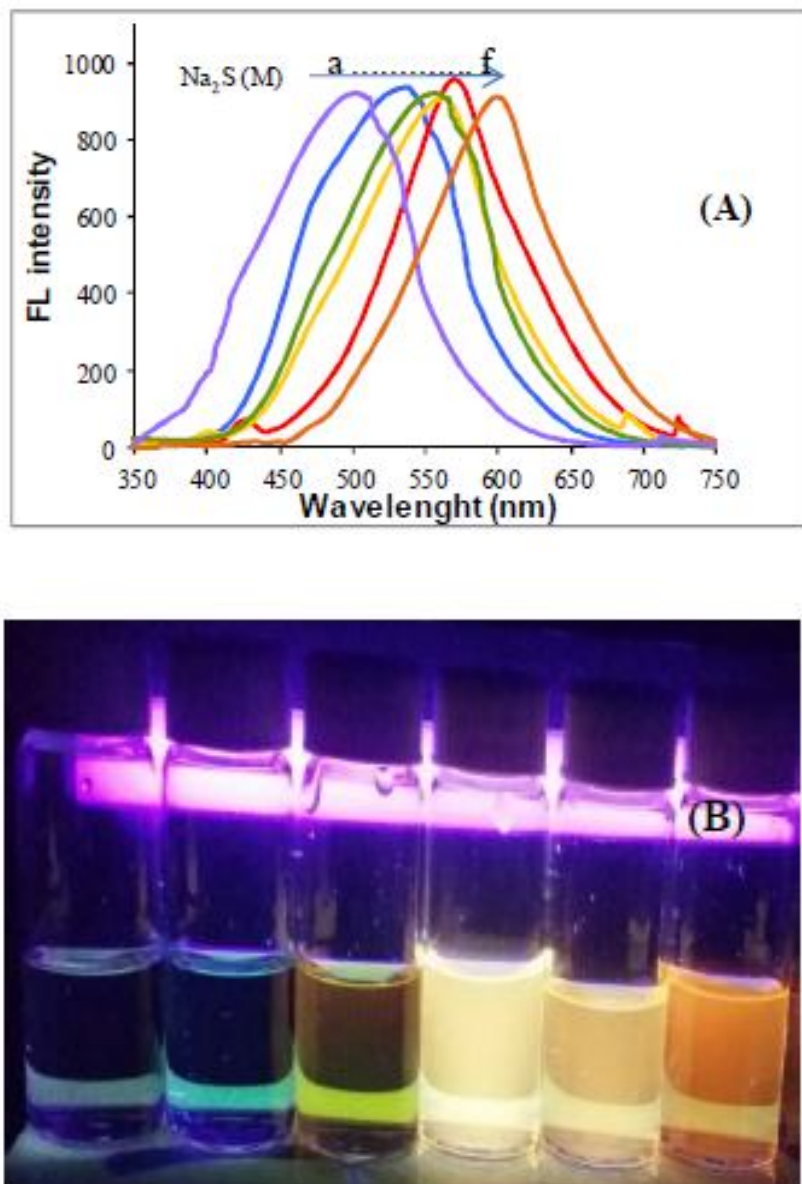


**Fig. 3.** (A) The fluorescence spectra of Cit-CdS QDs. From left to right, the concentrations of Na<sub>2</sub>S are a)  $4 \times 10^{-4}$ , b)  $8.5 \times 10^{-4}$ , c)  $1.5 \times 10^{-3}$ , d)  $2 \times 10^{-3}$ , e)  $4 \times 10^{-3}$  and f)  $6 \times 10^{-3}$  M. (B) Cit-CdS QDs irradiated with UV light. With the increase in Na<sub>2</sub>S concentrations the color of the light emitted changes from purple to orange.

leads to change the color of the solutions from violet to orange as the concentration of Na<sub>2</sub>S increases, implying an increase in particle size. In addition, the size and shape of the Cit-CdS QDs before and after adding MPN were

characterized by HRTEM as shown in (Fig. 4). From the TEM image, it was clearly seen that the Cit-CdS QDs used in this work are regular spherical nanocrystals with diameters ranging from 15-20 nm.

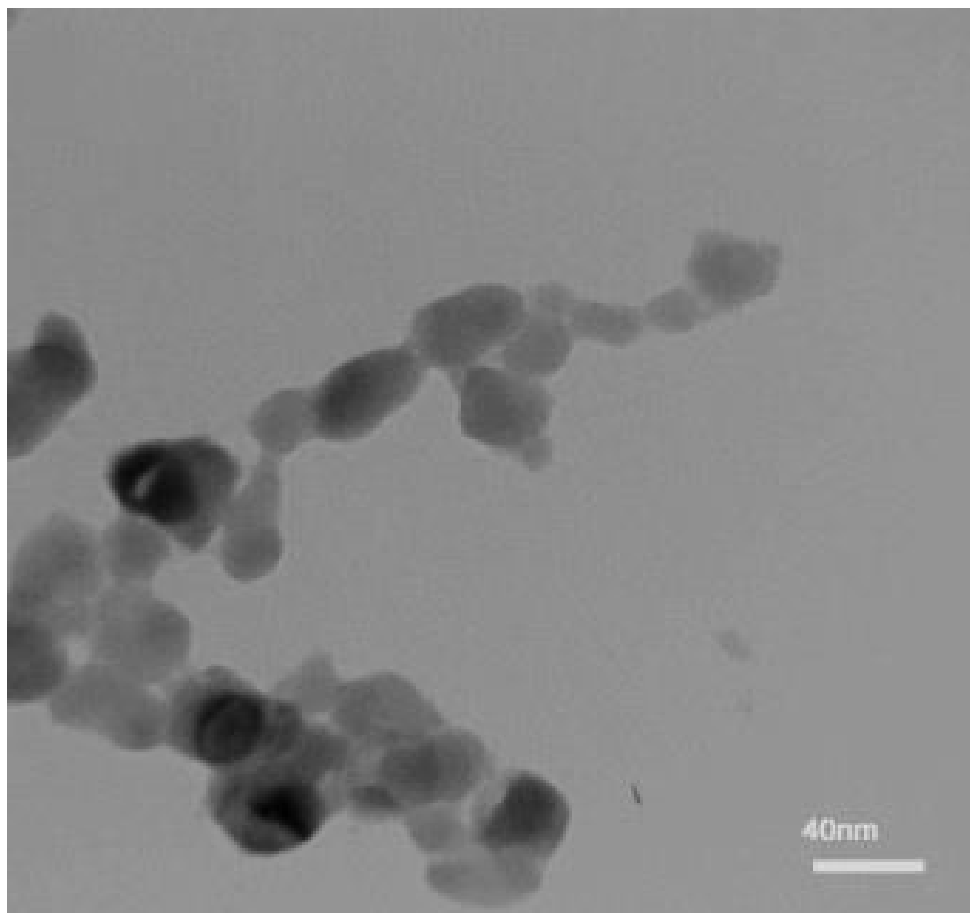


**Fig. 4.** TEM images of Cit-Capped CdS.

A, B and C show the IR spectra of Cit-CdS nanoparticles, meropenem and Cit-capped-CdS nanoparticles with meropenem, respectively (Fig. 5). The observed absorption peaks at  $3458.52\text{ cm}^{-1}$ ,  $1595\text{ cm}^{-1}$ ,  $1400\text{ cm}^{-1}$  and  $1078\text{ cm}^{-1}$  in the IR spectrum of (Fig. 5A) are attributed to OH, C=O, CH<sub>2</sub> and C-OH groups, respectively. In (Fig. 5B), peaks at  $3410\text{ cm}^{-1}$ ,  $2977\text{ cm}^{-1}$ ,  $1751\text{ cm}^{-1}$  and  $1386\text{ cm}^{-1}$  show OH, C-H, C=O and C-N groups, respectively. Peaks at  $3419\text{ cm}^{-1}$ ,  $2980\text{ cm}^{-1}$ ,  $836\text{ cm}^{-1}$  and two shoulders ( $x_1$  and  $x_2$ ) in (Fig. 5C) are evidence of interaction between Cit-capped-CdS nanoparticles with meropenem.

#### **The Influence of pH on Luminescence of Cit-capped CdS QDs**

The pH of the solution commonly had a strong effect on

the FL intensity of the QDs [38]. In order to select the optimum conditions for the determination of meropenem with the Cit-capped CdS QDs the effect of pH from 5 to 11 was studied using phosphate buffer solutions. It can be seen that (Fig. 6) pH influences the fluorescence intensity of QDs in the absence and presence of meropenem. Obviously, in pH = 6 meropenem greatly quenched the fluorescence intensity of CdS QDs. Thus, pH = 6 was selected for the subsequent studies.

#### **Effect of Reaction Time and Stability**

The reaction time was studied for the determination of meropenem in the room temperature and the results showed that 5 min after mixing MPN and Cit-CdS, Maximal quench fluorescence intensity was observed, and then the fluorescence signal was stable for at least 50 min. This

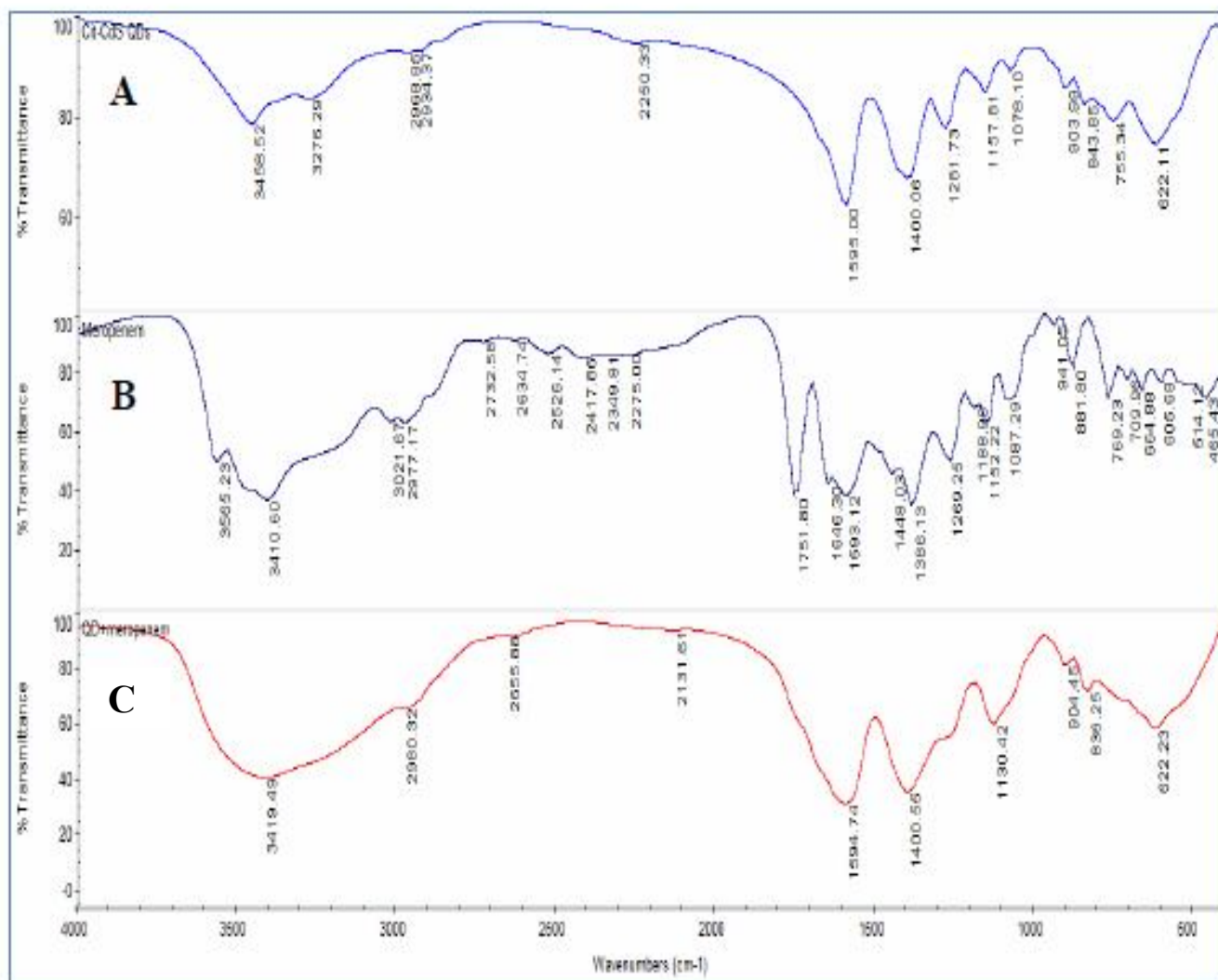


**Fig. 5.** The IR spectra of A) Cit-capped-CdS nanoparticles, B) MPN and C) Cit-capped-CdS nanoparticles with MPN.

showed the good stability of the detection system. Thus, the fluorescence was measured after 5 min of adding MPN to CdS QDs.

### Selectivity of the Sensor

To show the selectivity of the proposed sensor, the interference of ions including  $\text{Na}^+$ ,  $\text{K}^+$ ,  $\text{Co}^{2+}$ ,  $\text{Mg}^{2+}$ ,  $\text{Ca}^{2+}$ ,  $\text{Mn}^{2+}$ ,  $\text{Fe}^{2+}$  and some drugs such as (Ceftriaxone, Valsartan, Cetirizine, Ketotifen, Metronidazole, Cephalotin), *etc.*, that might be present in real samples, was investigated (Fig. 7). It was found that  $3.6 \times 10^{-4}$  M concentrations of anions and

drugs had little influence on the FL intensity of the quantum dots, while the concentration of MPN is  $3 \times 10^{-5}$  M.

### Detection of Meropenem by Quenching the Fluorescence of Cit-capped CdS QDs

The fluorescence intensity of the Cit capped CdS QDs reduced by the adding MPN indicating an interaction between the QDs and MPN that results in fluorescence quenching (Fig. 8a). The mechanism of the fluorescence quenching process was investigated using Stern-Volmer equation [37], given by the following equation:

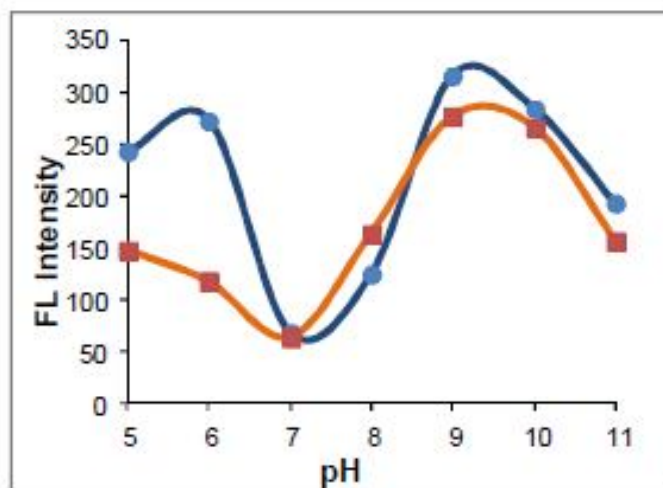


**Fig. 6.** (A) Effects of pH on the of fluorescence of QDs: the two curves represent the fluorescence intensity of QDs before (●) and after (■) the addition of MPN. The concentration of phosphate buffer solution and MPN were 0.1 M and  $3.3 \times 10^{-4}$  M, respectively.

$$I_0/I = K_{SV}C + I$$

$I_0$  and  $I$  are the fluorescence intensity in the absence and the presence of meropenem, respectively,  $C$  is the meropenem concentration and  $K_{SV}$  is quenching constant of the Stern-Volmer equation. Under the optimum condition, the resulting plot (Fig. 8b) shows a good linear dependence in the range of  $6 \times 10^{-10}$ - $2.1 \times 10^{-3}$  M with a determination coefficient of 0.9966. For low meropenem concentration, a linear Stern-Volmer relationship between  $I/I_0$  and  $[C]$  can be observed. This can signify that at these concentrations the mechanism was based on the meropenem binding on the surface of QDs simulating recombination centers for holes and electrons that make quenching of QDs fluorescence. The detection limit (LOD), was calculated using the equation  $3\sigma/S$  ( $\sigma$  standard deviation of blank measurements of 6 repetitions and  $S$  calibration curve slope) of 0.5 nM. No emission peak wavelength shift was found even at relatively high concentrations of meropenem.

A comparison between this method and some other methods reported recently for the determination of meropenem is presented in Table 2. The present method showed a lower detection limit and wider linear range and hence this method is very simple and selective toward meropenem.

### Measuring Meropenem in Real Samples

To gauge the validity of our method for real sample analyses, the urine sample was used as a clinical sample model. The results of chromatography and spectrophotometric methods are shown in Table 3. Good recovery for the determination of MPN was obtained, thus the validity of the proposed method for direct analysis of MPN in real sample was confirmed. Optimized HPLC conditions are summarized in Table 1, and an average peak with retention time of 4.32 is shown in (Fig. 9).

### CONCLUSIONS

In this work, Cit-capped CdS QDs were successfully synthesized and used as a sensitive and selective fluorescence probe for detection of meropenem. In the presence of meropenem, the fluorescence intensity of Cit-CdS QDs was decreased as the concentration of MPN increased. The fabricated sensor has good selectivity and sensitivity compared to other tested drugs and metal ions for determination of MNP. Additionally, this nanosensor has been successfully applied for the determination of meropenem in real samples under the optimum conditions. Therefore, this method can be provided with an excellent selectivity and sensitivity for the fast, simple and accurate

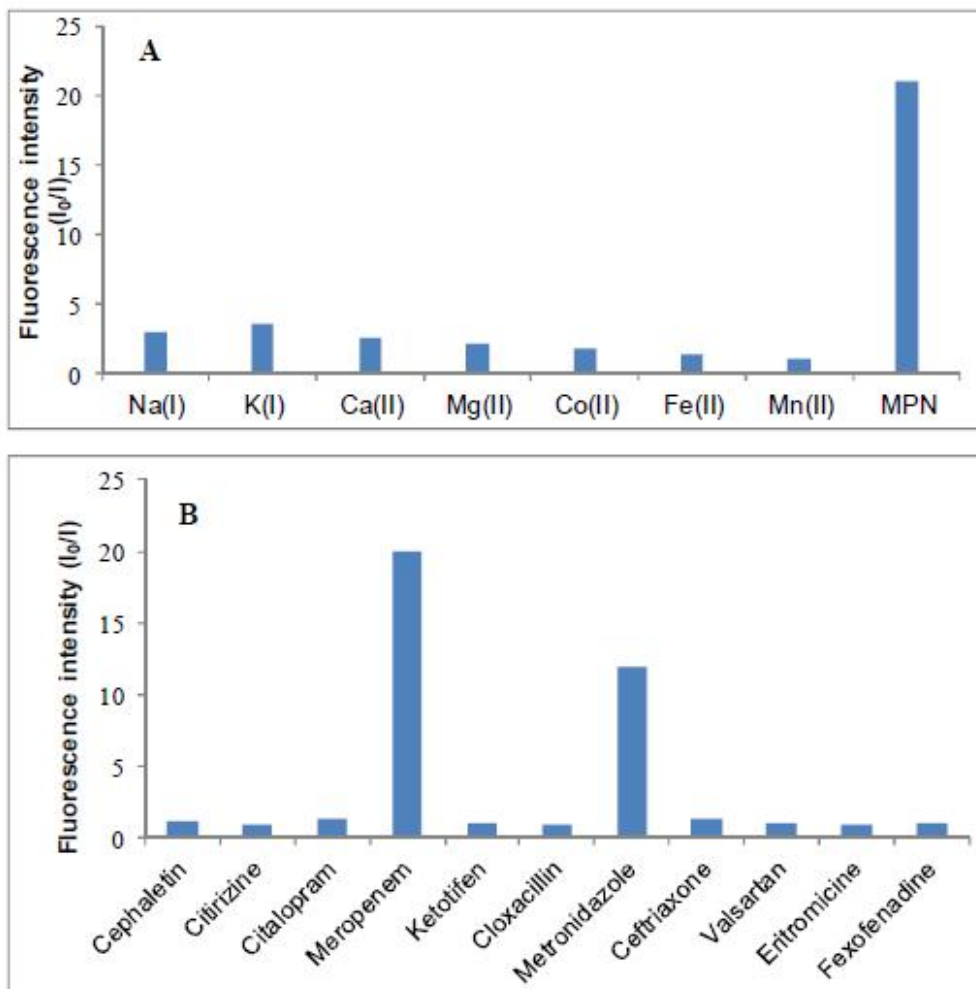


**Fig. 7.** Effect of A) ions, and B) drugs on the luminescence of Cit-Capped CdS. Concentrations of ions and drugs are all  $3.6 \times 10^{-4}$  M, and MPN is  $3 \times 10^{-5}$  M.

**Table 2.** Comparison of the Performances of Different Methods

Methods	Linear range	Detection limits	Ref.
	(M)	(M)	
SPE-LC	$1.3 \times 10^{-5}$ - $2.6 \times 10^{-4}$	$6.5 \times 10^{-6}$	[34]
HPLC	$2.6 \times 10^{-3}$ - $2.6 \times 10^{-1}$	$2.6 \times 10^{-4}$	[40]
HPLC	$5.2 \times 10^{-8}$ - $1.3 \times 10^{-4}$	-	[41]
CE	$5.2 \times 10^{-5}$ - $2.6 \times 10^{-1}$	$5.2 \times 10^{-3}$	[42]
CZE	$1.3 \times 10^{-3}$ - $5.2 \times 10^{-1}$	-	[43]
This method	$6 \times 10^{-10}$ - $2.1 \times 10^{-3}$	$5.2 \times 10^{-9}$	-



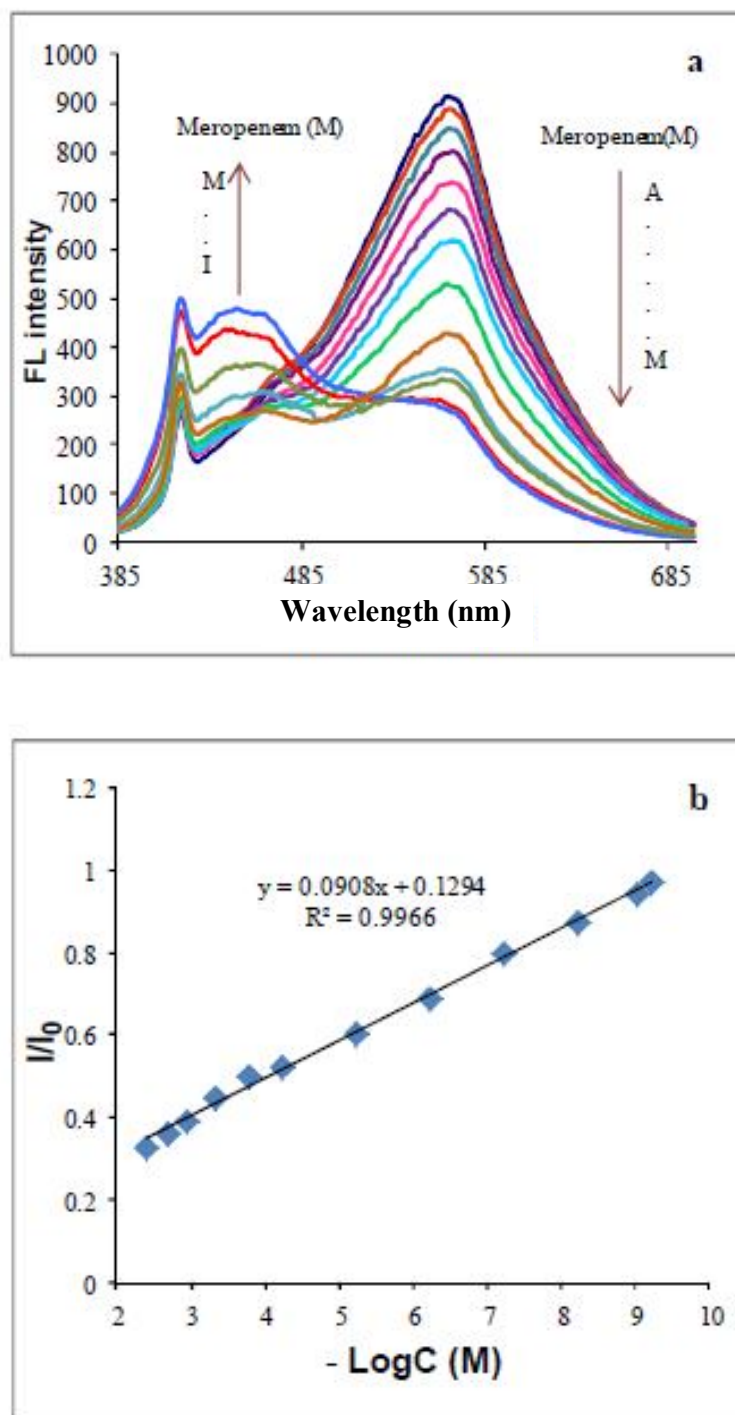


**Fig. 8.** (a) Fluorescence spectra of Cit-CdS QDs in the presence of meropenem. From top to bottom, the concentrations of MPN were A) 0 B)  $6 \times 10^{-10}$  C)  $9 \times 10^{-10}$  D)  $6 \times 10^{-9}$  E)  $6 \times 10^{-8}$  F)  $6 \times 10^{-7}$  G)  $6 \times 10^{-6}$  H)  $6 \times 10^{-5}$  I)  $1.6 \times 10^{-4}$  J)  $5 \times 10^{-4}$  K)  $1.1 \times 10^{-3}$  L)  $1.8 \times 10^{-3}$  M)  $2.1 \times 10^{-3}$  M (b) Langmuir-binding isotherm relationship between FL enhancement and MPN.

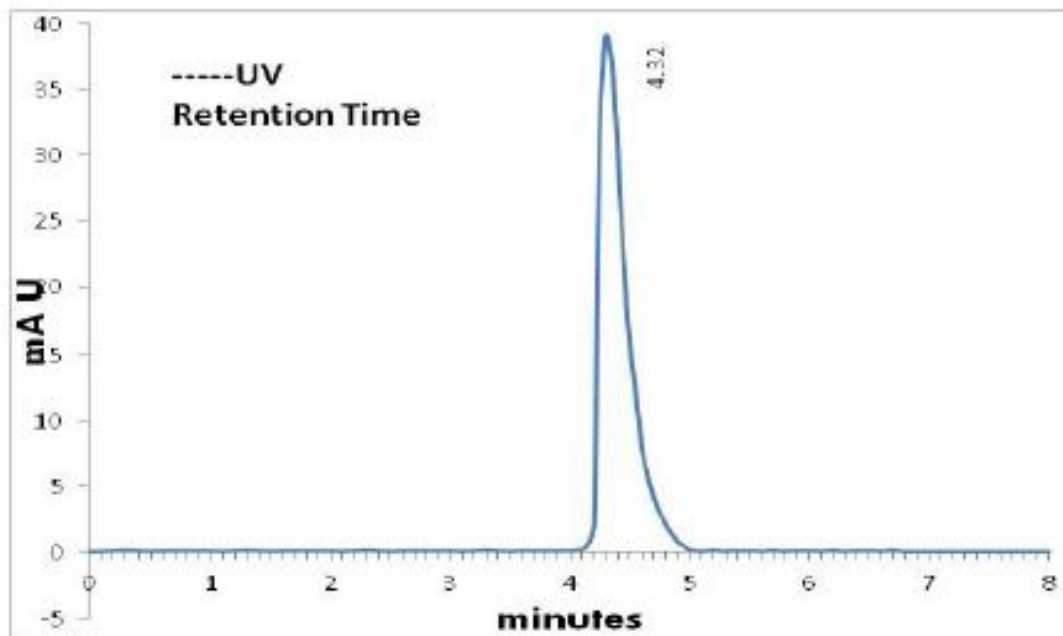


**Fig. 9.** The chromatogram of MNP (200 mg), with 0.2% triethylamine pH 6 water: Acetonitrile (20:80).

**Table 3.** Determination of Meropenem in Urine Samples

Method	The amount present in the mixture	The amount added ( $\mu\text{M}$ )	The amount found ( $\mu\text{M}$ )	The percent of drug recovered	RSD
Chromatography	-	6	5.9	98.3	2.2
Spectrofluorimetry	-	4	4.1	102.5	2.1

Mean percentage of recovery was calculated for five replicate determinations.

detection of trace amounts of meropenem in real samples.

## REFERENCES

- [1] Y. Du, B. Xu, T. Fu, M. Cai, F. Li, Y. Zhang, Q. Wang, *J. Am. Chem. Soc.* 132 (2010) 1470.
- [2] T. Tang, L. Lee, S. Achilefu, *J. Am. Chem. Soc.* 134 (2012) 4545.
- [3] C. Frigerio, D.S.M. Ribeiro, S.S.M. Rodrigues, A. V.L.R.G. Abreu, B.J.A.C. Barbosa J.A.V. PriorK. L. Marques, J.L.M. Santos, *Anal. Chim. Acta* 735 (2012) 9.
- [4] C.W. Chan, J. Maxwell, S. Nie, *Curr. Opin. Biotech.* 13 (2002) 40.
- [5] E.M. Ali, Y. Zheng, H. h. Yu, J.Y. Ying, *Anal. Chem.* 79 (2007) 9452.
- [6] J.R. Lakowicz, I. Gryczynski, Z. Gryczynski, C.J. Murphy, *J. Phys. Chem. B* 103 (1999) 7613.
- [7] R.H. Yang, W.H. Chan, K.A. Li, *J. Am. Chem. Soc.* 125 (2003) 2884.
- [8] Y. Bao, J. Li, J. Zhu, *Chin. Chem. Lett.* 22 (2011) 843.
- [9] T. Ye, S. Lu, J. Wang, J. Lu, *Chin. Chem. Lett.* 22

- (2011) 1253.
- [10] Y. Chen, Z. Rosenzweig, *Anal. Chem.* 74 (2002) 5132.
- [11] Y. Shang, F. Wu, *Microchim. Acta* 177 (2012) 333.
- [12] M. Koneswaran, R. Narayanaswamy, *Sens. Actuators B* 139 (2009) 104.
- [13] Y.S. Xia, C.Q. Zhu, *Talanta* 75 (2008) 215.
- [14] R. Gill, R. Freeman, J.P. Xu, I. Willner, S. Winograd, I. Shweky, U. Banin, *J. Am. Chem. Soc.* 128 (2006) 15376.
- [15] Z. Zhelev, R. Bakalova, H. Ohba, R. Jose, Y. Imai, Y. Baba, *Anal. Chem.* 78 (2006) 321.
- [16] T. Jin, F. Fujii, E. Yamada, Y. Nodasaka, M. Kinjo, *J. Am. Chem. Soc.* 128 (2006) 9288.
- [17] I.L. Medintz, H.T. Uyeda, E.R. Goldman, H. Mattoussi, *Nat. Mater.* 4 (2005) 435.
- [18] D.R. Larson, W.R. Zipfel, R.M. Williams, S.W. Clark, M.P. Bruchez, F.W. Wise, W.W. Webb, *Science* 300 (2003) 1434.
- [19] M. Hou, J. Na, *Anal. Bioanal. Chem.* 397 (2010) 3589.
- [20] L. Guo, J. Zhong, J. Wu, F.F. Fu, G. Chen, X. Zheng, S. Lin, *Talanta* 82 (2010) 1654.
- [21] Z. He, H. Zhu, P. Zhou, *J. Fluoresc.* 22 (2012) 193.
- [22] N. Samadi, S. Masoum, B. Mehrara, H. Hosseini, *J. Chromatogr. B* 1001 (2015) 75.
- [23] N. Samadi, S. Narimani, *Spectrochim. Acta, Part A* 163 (2016) 8.
- [24] S.C. Sowmith, B. Yadagiri, Y.L.N. Murthy, T. Krishna Mohan, *Pharm. Res.* 12 (2018) 378.
- [25] C. Akay, S. Ozkan, Z. Senturk, S. Cevheroglu, *Farmaco* 57 (2002) 953.
- [26] M. Farré, I. Ferrer, A. Ginebreda, M. Figueras, L. Olivella, L. Tirapu, M. Vilanova, D. Barceló, *J. Chromatogr. A* 938 (2001) 187.
- [27] M.A. Pfaller, R.N. Jones, *Microbiol. Infect. Dis.* 28 (1997) 157.
- [28] J.L. Blumer, *Int. J. Antimicrob. Agents* 8 (1997) 73.
- [29] L.R. Wiseman, A.J. Wagstaff, R.N. Brogden, H.M. Bryson, *Drugs* 50 (1995) 73.
- [30] J.S. Bradley, *Infect. Dis. J.* 16 (1997) 263.
- [31] S. Bompadre, L. Ferrante, M. De Martinis, L. Leone, *J. Chromatogr. A* 812 (1998) 249.
- [32] M. Ehrlich, F.D. Daschner, K.K. Ummerer, *J. Chromatogr. B* 751 (2001) 357.
- [33] Y. O'zkan, I. Ku'cu'kgu'zel, S.A. O'zkan, Aboul-Eneim, *Biomed. Chromatogr.* 15 (2001) 263.
- [34] C. Robotel, T. Buclin, P. Eckert, M.D. Schaller, J. Biollaz, L.A. Decosterd, *J. Pharm. Biomed. Anal.* 29 (2002) 17.
- [35] S. Taniguchi, K. Hamase, A. Kinoshita, K. Zaitso, *J. Chromatogr. B* 727 (1999) 219.
- [36] A.S.L. Mendez, M. Steppe, E.E.S. Schapoval, *J. Pharm. Biom. Anal.* 33 (2003) 947.
- [37] G.L. Wang, Y.M. Dong, H.X. Yang, Z.J. Li, *Talanta* 83 (2011) 943.
- [38] D.A. Skoog, F.J. Holler, T.A. Nieman, *Principles of Instrumental Analysis*, 7th ed., Saunders College, Philadelphia (1998) 601.
- [39] S. Shuang, J. Qiu, *Acta Phys. Chim. Sin.* 25 (2009) 1342.
- [40] S. Bompadre, L. Ferrante, M. De Martinis, L. Leone, *J. Chromatogr. A* 812 (1998) 249.
- [41] D. Farin, R. Kitzes-Cohen, G. Piva, I. Gozlan, *Chromatographia* 49 (1999) 253.
- [42] T. Kitahashi, I. Furuta, *J. Chromatogr.* 43 (2005) 430.
- [43] Y. Mrestani, R. Neubert, F. Nagel, *J. Pharm. Biomed. Anal.* 20 (1999) 899.